



AMERICAN UNIVERSITY OF BEIRUT

EXPERIMENTAL AND NUMERICAL STUDY OF BACK-COOLING  
CAR SEAT SYSTEM USING EMBEDDED HEAT PIPES TO  
IMPROVE PASSENGER'S COMFORT

by  
OMAR BADRI HATOUM

A thesis  
submitted in partial fulfillment of the requirements  
for the degree of Master of Engineering  
to the Department of Mechanical Engineering  
of the Faculty of Engineering and Architecture  
at the American University of Beirut


Beirut, Lebanon  
April 2017


AMERICAN UNIVERSITY OF BEIRUT

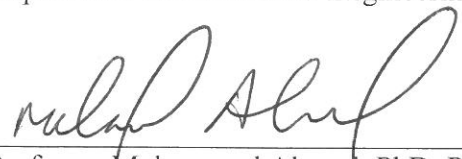
Experimental and Numerical Study of Back-Cooling Car-Seat System  
Using Embedded Heat Pipes to Improve Passenger's Comfort

by  
OMAR BADRI HATOUM

Approved by:

  
\_\_\_\_\_  
Professor Nesreene Ghaddar, PhD, Professor  
Department of Mechanical Engineering  
Advisor

  
\_\_\_\_\_  
Professor Kamel Abu Ghali, PhD, Professor  
Department of Mechanical Engineering  
Co-Advisor

  
\_\_\_\_\_  
Professor Mohammad Ahmad, PhD, Professor  
Department of Chemical Engineering  
Member of Committee

Date of thesis/dissertation defense: April 11, 2017

# AMERICAN UNIVERSITY OF BEIRUT


## THESIS, DISSERTATION, PROJECT RELEASE FORM

Student Name: Hatoum Omar Badri  
Last First Middle

Master's Thesis       Master's Project       Doctoral Dissertation

I authorize the American University of Beirut to: (a) reproduce hard or electronic copies of my thesis, dissertation, or project; (b) include such copies in the archives and digital repositories of the University; and (c) make freely available such copies to third parties for research or educational purposes.

I authorize the American University of Beirut, to: (a) reproduce hard or electronic copies of it; (b) include such copies in the archives and digital repositories of the University; and (c) make freely available such copies to third parties for research or educational purposes after : **One ---- year from the date of submission of my thesis, dissertation, or project.**  
**Two ---- years from the date of submission of my thesis, dissertation, or project.**  
**Three ---- years from the date of submission of my thesis, dissertation, or project.**

 May 8 2017  
Signature Date

## ACKNOWLEDGMENTS

I would like to thank my advisors Professor. Nesreene Ghaddar and Professor Kamel Abu Ghali for their guidance, recommendations and thoughtful ideas.

I would also like to show deep gratitude and appreciation to Dr. Nagham Ismail for her thoughtful ideas in the Mathematical formulation.

Special thanks to my family members and friends for their support throughout the years.

# AN ABSTRACT OF THE THESIS OF

Omar Badri Hatoum for Master of Engineering  
Major: Mechanical Engineering

Title: Experimental and Numerical Study of Back-Cooling Car-Seat System Using Embedded Heat Pipes to Improve Passenger's Comfort

This work develops a back-cooling system for a car seat using seat embedded heat pipes to improve passenger comfort. The heat pipe system utilizes the temperature difference between the passenger back and the car cabin air to remove heat from the human body and enhance the comfort state. The developed seat heat-pipe model was validated experimentally using a thermal manikin with controlled constant skin temperature mode in a climatic chamber. Good agreement was found between the measured and the numerically predicted values of base panel temperature.

By integrating the validated heat pipe with a bio-heat model, the back segmental skin temperature as well as the overall thermal comfort was predicted and compared with the conventional seat case without the heat pipe system. The heat pipes were able to reduce the skin temperature by 1 °C and to increase the overall thermal comfort of the body by 30 %. In addition, a parametric study was performed to determine the optimal number of heat pipes that ensure the thermal comfort of the passenger.

# CONTENTS

ACKNOWLEDGMENTS.....	v
ABSTRACT.....	vi
LIST OF NOMENCLATURE.....	viii
LIST OF ILLUSTRATIONS.....	ix
LIST OF TABLES.....	X

## Chapter

I. INTRODUCTION AND SYSTEM DESCRIPTION.....	1
A. Introduction.....	1
B. System Description.....	4
II. DEVELOPMENT OF MATHEMATICAL FORMULATION AND ITS COUPLING WITH BIO-HEAT MODEL.....	6
A. Mathematical Formulation.....	6
B. Discretization of Equations and Numerical Methodology of heat pipe model .....	10
C. Integration of The Bio-heat Model With The Heat Pipe Model.....	11
III. EXPERIMENTAL METHODOLOGY.....	15
A. Experimental Setup.....	15
B. Contact Resistance Measurement .....	17
C. Experimental Protocol of The Heat Pipe System.....	17
IV. RESULTS AND DISCUSSIONS.....	19
A. Validation of The Heat Pipe Model With Experimental Data.....	19
B. Integrated Bio-heat model and Heat Pipe Model.....	20
C. Parametric study using validated bio-heat model and heat pipe model.....	21

D. Conclusion.....24

**BIBLIOGRAPHY.....26**



## NOMENCLATURE

$A$	: Area ( $\text{m}^2$ )
$D$	: Diameter (m)
$h$	: Heat transfer coefficient ( $\text{W}/\text{m}^2\cdot\text{k}$ )
$K$	: Conductivity ( $\text{W}/\text{m}\cdot\text{K}$ )
$L$	: Length (m)
$R$	: Resistance ( $\text{K}/\text{W}$ )
$T$	: Temperature (K)
$q$	: Heat flux ( $\text{W}/\text{m}^2$ )
$g$	: Gravitational acceleration ( $\text{m}/\text{s}^2$ )

### Greek letters

$\delta$	: Thickness (m)
$\Theta$	: Angle (degree)
$\rho$	: Density ( $\text{kg}/\text{m}^3$ )

### Subscripts

$a$	: Ambient air
$b$	: Base panel
$s$	: Back skin
$i$	: Base panel nodes
$j$	: Nodes on heat pipe
$o$	: Outer
$p$	: Heat pipe
$l$	: Liquid
$v$	: Vapor
$sat$	: Saturated
$ins$	: Thermal insulating material
$bi$	: Differential grid of the base panel
$contact$	: Contact between base panel and the skin surface layer
$ad$	: Adhesive layer
$con$	: Condenser section of heat pipe
$eva$	: Evaporator section of heat pipe
$wick$	: Wick of the heat pipe

# ILUSTRATIONS

Figure

- 1: Schematic diagram of heat pipe system (a) with the human being sitting on the car seat (b) including front view, side and plan.....5
- 2: Differential grid partition of the base panel.....6
- 3: Flow chart of the coupling methodology.....14
- 4: (a) Front view of thermal manikin (b) Side view of thermal manikin.....16
- 5: Manufactured heat pipe geometry.....16
- 6: Heat pipe assembly (a) with insulation layer (b) without insulation layer .....18
- 7: Results as a function of the number of heat pipes (a) Local thermal comfort and local thermal sensation (b) Overall thermal comfort.....24

# TABLES

Table

1: Thermal resistances of the heat balance equations	<b>Error! Bookmark not defined.</b>	9
2: Thermal properties of the heat pipe	<b>Error! Bookmark not defined.</b>	18
3: Temperature of the base panel evaluated experimentally and theoretically with and without heat pipe		19
4: Results of the back skin temperature, local thermal comfort, and the thermal sensation with and without heat pipe.		20
5: Temperature of the base panel and the back skin surface as a function of the number of heat pipes.		23



# CHAPTER I

## INTRODUCTION AND SYSTEM DESCRIPTION

### **A. Introduction**

Seats, in general, hinder the heat and moisture transport from the human back to the environment bringing thermal discomfort for a seated person. The torso of a seated person is well exposed to convective air flow whereas the pelvis and the back are well surrounded with the seat structure material. In fact, a seated person dissipates heat from the back which increases the temperature of the chair and adversely rises the temperature of the back (H. Zhang; E. Arens; C. Huizenga and T. Han, 2010) Therefore, moisture accumulation can occur at the back affecting thermal comfort. Lindsay et al. (R. Lindsay, 1977) reported that taxi drivers, truck drivers, bus drivers, and other persons who drive a motor vehicle for an extended period of time are exposed to different kinds of risks and discomfort which adversely affect their working performance.

In non-uniform environments such as those encountered by car passengers, the human body may experience a wide range of physical parameters that would make the conventional methods (PMV) for computing the human state of comfort inapplicable and would necessitate the computation of the local segmental comfort to determine the overall state comfort of the occupant. The concept of local segmental body cooling started in office building and it was found that substantial energy savings can be achieved when targeting the upper body segments (H. Zhang; E. Arens; C. Huizenga and T. Han, 2010) (M. Itani; D. Ouahrani; N. Ghaddar; K. Ghali; and W. Chakroun, 2016) (W. Hweij,; N. Ghaddar; K. Ghali and C. Habchi. 2016). In fact, this concept for local cooling of seated passengers can be exploited to improve passenger

comfort. Zhang et al. (H. Zhang; E. Arens; C. Huizenga and T. Han, 2010) reported that providing local segmental cooling is a significant aspect that triggers a state of thermal comfort especially cooling the back segment of a seated passenger because the back is one of the body segments that is very sensitive to cooling. Besides, according to Corter et al. (J. Cotter and N. Taylor 2005), the back temperature has the highest coefficient (28%) compared to chest coefficient (8%) in determining the mean skin body temperature used in overall thermal comfort estimation. Moreover, Itani et al. (M. Itani; D. Ouahrani; N. Ghaddar; K. Ghali; and W. Chakroun, 2016) studied the effect of cooling vests on the torso segment by using phase change materials (PCM) and they reported that placing the PCM cooling vests on the torso segment improved the overall thermal comfort by 94 %.

Several techniques have been implemented by researchers to cool the back of a seated person in a way that enhances the person's overall thermal comfort (W. Rock; E. Dionne; C. Haryslak; W. Lie and G.Vainer, 2007) (W. Zheng and Z. Guo, 2012). Some researchers have used simple methods such as plaited double-knit fabric in offices in a fashion that increased the contact area with air (W. Rock; E. Dionne; C. Haryslak; W. Lie and G.Vainer, 2007). This method enhanced convective cooling of the human back and increased the transfer of moisture away from the skin. However, the plaited double-knit fabric is not applicable in all seats especially car seats, since car seats are rigid and have a structural support. Others have used a portable cooling pad for seats to cool the back of a seated person (W. Zheng and Z. Guo, 2012). This is based on designing a contoured surface that includes concave and convex sections accompanied by a fan that draws air and cools the back. Nevertheless, the portable cooling pad is not considered as a passive system because it includes operating cost associated with the fan rotation. Consequently, it is of interest to design a passive cooling system that can be easily embedded in car seats.

Heat pipe system is a common passive cooling system used in many applications. It is a heat transfer device that does not have any moving parts and it is applicable with relatively low temperature difference between the heat source and the heat sink. Its effectiveness has been thoroughly studied in the literature for different applications: solar water heater (S. Chen and J. Yang, 2016) (E. Azad, 2008), high power electronic components cooling (L. Vasiliev; D. Lossouarn; C. Romestant; A. Alexandre; Y. Bertin; Y. Piatsiushyk and V. Romanenkov, 2009), and photovoltaic thermal panel (A. Sweidan; N. Ghaddar and K. Ghali, 2016). Moreover, heat pipe systems have been studied in HVAC applications for improving heat recovery in a narrow temperature difference of approximately 10 °C (X. Wu; P. Johnson and A. Akbarzadeh, 1997) (H. Chaudhry and B. Hughes, 2014).. In addition to its effectiveness in cooling, heat pipe system excludes any moving part and could be easily embedded in car seats. Such new application needs further investigation given the narrow range of temperature difference between the back and the compartment air. Thus, it is of interest to study the performance of the heat pipe system in cooling the car seat and in providing the human comfort at no additional energy cost. To the authors' knowledge, car seat heat pipe system has never been studied in literature or has been commercially produced.

In order to assess thermal comfort provided by the heat pipe system embedded in the car seat, a bio-heat model that is capable of studying the physiological response of the human body is needed. Several researchers have integrated their models of cooling and ventilation systems with bio-heat models. Itani et al. (M. Itani; D. Ouahrani; N. Ghaddar; K. Ghali; and W. Chakroun, 2016) integrated a fabric-PCM model with a bio-heat model (M. Salloum; N. Ghaddar and K. Ghali, 2007) to improve the design of the PCM cooling vest taking into consideration the human physiology at high metabolic rates in hot environments. Moreover, Hweij et al. (W. Hweij,; N.

Ghaddar; K. Ghali and C. Habchi. 2016) studied the performance of displacement ventilation aided with chair fans, and coupled the model with a bio-heat model (M. Salloum; N. Ghaddar and K. Ghali, 2007) to study the human thermal response. Since a seated person is subject to non-uniformity in environment due to the direct contact of the back with the car-seat surface, the segmental Bio-heat model should be sensitive to this non-uniformity. To determine the physiological and the thermal response of the human body in non-uniform environment, the bio-heat model of Othmani et al. (M. Al-Othmani; N. Ghaddar and K. Ghali, 2008) considered angular variation in skin temperature for the trunk segments, the upper limbs, and the lower limbs which improved the segmental Bioheat model of Salloum et al. (M. Salloum; N. Ghaddar and K. Ghali, 2007).

Therefore, the objective of this study is to determine the feasibility of embedding the heat pipe system in the car seat and its effect on reducing the thermal discomfort of the human body. In other words, it is aimed to passively improve the comfort of passengers without the need of lowering the temperature setting inside the car. This is achieved by (i) developing a mathematical model that predicts the performance of heat pipe system; (ii) validating the model by performing an experiment on a thermal manikin placed on a car seat embedded with heat pipes; (iii) integrating the heat pipe model with a bio-heat model to simulate the thermal human response; and (iv) developing a parametric study to determine the optimum number of heat pipes in the suggested system.

## **B. System Description**

In this study, a heat pipe system is used to absorb the heat from the back and dissipate it to the environment. In the evaporator section, the heat pipes are attached from one side to an aluminum plate that ensures good contact area and significant conductive heat transfer with the human



back. On the other side, the evaporator section is backed with good thermal insulation material to ensure that heat transfer takes place only between the human back and the evaporator heat pipe section and is not lost to the environment but is carried to the condenser section. At the condenser section, the heat pipes are exposed to the car compartment environment. The assembly, which is composed of the aluminum plate, the heat pipes, and the thermal insulation, is fixed to the car seat using a clamp support. It is worth to note that the lateral parts of the assembly are also insulated. The setup of the system between the human back and the car seat is presented in Fig. 1(a) and Fig. 1(b).

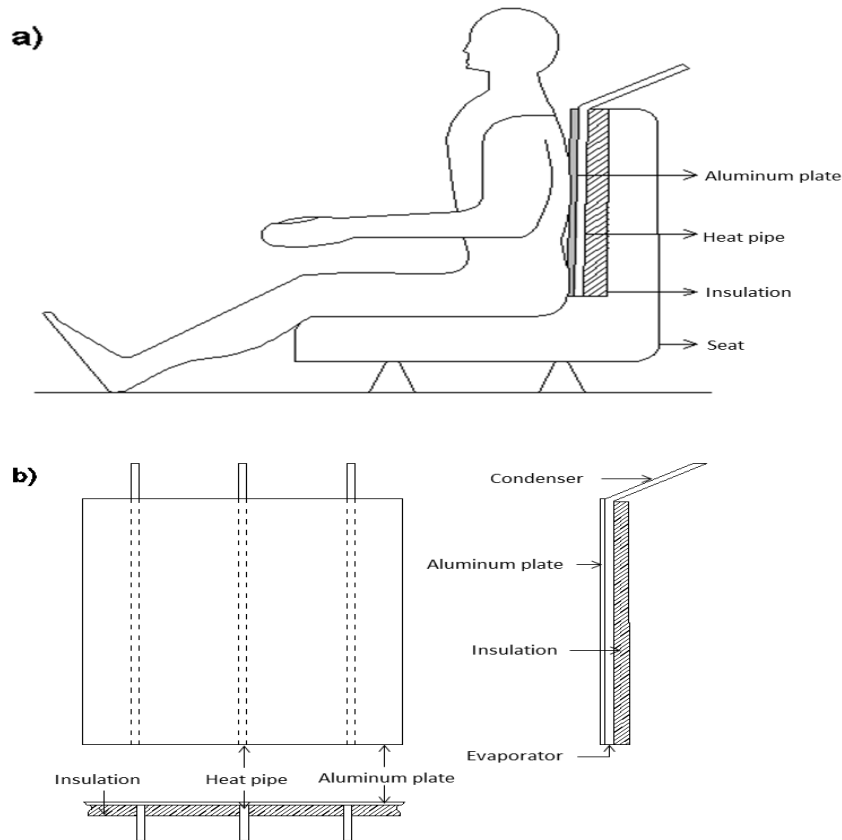


Fig. 1 Schematic diagram of heat pipe system (a) with the human being sitting on the car seat (b) including front view, side, and plan

## CHAPTER II

# DEVELOPMENT OF THE MATHEMATICAL MODEL AND ITS COUPLING WITH BIO-HEAT MODEL

### A. Mathematical Formulation

A mathematical model was developed to predict the performance of heat pipe system that is used to cool the back of a seated driver. The heat pipe model is composed of four simplified steady-state heat transfer equations that were developed to determine the temperature of the base panel. In order to find the human back skin temperature, a bio-heat model is integrated to the heat pipe model (M. Al-Othmani; N. Ghaddar and K. Ghali, 2008). This segmental bio-heat model should be able to predict the physiological and thermal response of the human body for given metabolic rate, clothing resistance, and local environmental conditions adjacent to each clothed segment.

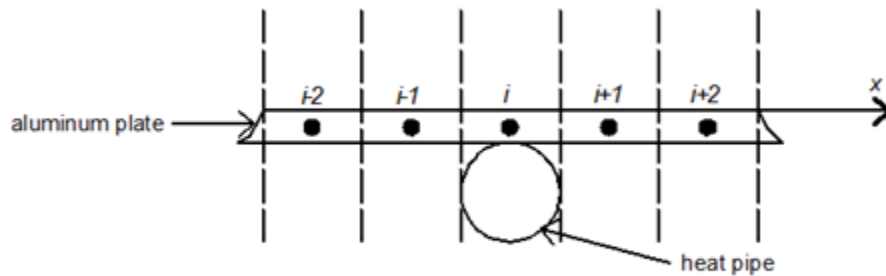


Fig. 2. Differential grid partition of the base panel

The plate consists of several nodes divided into two types: the heat pipe nodes and the non-heat pipe (middle) nodes as represented in Fig. 2. The heat pipe nodes represent the part of the aluminum plate that is in direct contact with the heat pipe. Thus, they absorb heat from the heat source and transport it to the evaporator section causing the refrigerant to boil. However, the

non-heat pipe nodes represent the part of the aluminum plate that is not in contact with the heat pipe. These nodes are insulated from one side and exposed to the heat source from the other side as shown in Fig. 2.

The energy equations of the base panel and the heat pipe were developed by Gang et al. (P. Gang; F. Huide; Z. Tao and J. Jie 2011) and used by Sweidan et al. (A. Sweidan; N. Ghaddar and K. Ghali, 2016) to study the effectiveness of heat pipe photovoltaic thermal system with phase change material for thermal storage. In this study, a model of heat pipe system is developed. The mathematical model consists of four heat balance equations, two of which are for the base panel and the other two for the heat pipe. To simplify the mathematical model, some assumptions are made as follows:

- The heat conduction of the aluminum plate in the longitudinal and normal directions is neglected
- The heat balance equations are considered under steady state condition since all the input parameters (skin temperature and ambient conditions) are constant with respect to time.

Taking into consideration these assumptions, the steady state heat balance equation for the heat pipe node is given by

$$\frac{K_b \partial^2 T_b}{\partial x^2} \times A_{bi} \cdot \delta_b + \frac{(T_a - T_b)}{R_{b,a}} + \frac{(T_{p, \text{evap}} - T_b)}{R_{p,b}} + \frac{(T_s - T_b)}{R_{\text{contact}}} \times A_{bi} = 0 \quad (1)$$

where  $R_{p,a}$  and  $R_{p,b}$  represent respectively the thermal resistance between the base panel and the ambient air and the thermal resistance between the aluminum plate and the heat pipe (see Table 1);  $R_{\text{contact}}$  represents the contact resistance between the back skin surface and the base panel is estimated experimentally (refer to the experiment section).

The first term of equation (1) is the net heat conducted along the x-direction of the aluminum plate as shown in Fig. 2. The second term is the heat transferred between the base panel and the environment. The third term is the heat transferred between the evaporator section and the base panel. Finally, the fourth term is the heat transferred between the back skin and the base panel.

The steady state heat balance equation of the middle node is given by

$$\frac{K_b \partial^2 T_b}{\partial x^2} \times A_{bi} \cdot \delta_b + \frac{(T_a - T_b)}{R_{b,a}} + \frac{(T_s - T_b)}{R_{contact}} \times A_{bi} = 0 \quad (2)$$

The heat balance equation of the evaporator section is given by

$$\frac{(T_{\rho,con} - T_{\rho,eva})}{R_{eva,con}} + \frac{(T_b - T_{\rho,eva})}{R_{\rho,b}} = 0 \quad (3)$$

where  $R_{eva,con}$  is the total thermal resistance of the heat transferred between the evaporator section and the condenser section as summarized in table 1. The temperature gradient of the working fluid along the axial length of the heat pipe can be disregarded, since the vapor space is regarded to operate at a fixed saturation pressure. The first term of equation (3) is the heat transmitted between the evaporator section and the condenser section while the second term is the heat transferred between the evaporator section and the base panel.

The steady state heat balance equation of the condenser section is given by

$$\frac{(T_a - T_{\rho,con})}{R_{con,a}} + \frac{(T_{\rho,eva} - T_{\rho,con})}{R_{eva,con}} = 0 \quad (4)$$

The first term of equation (4) represents the heat loss by natural convection to the environment in the condenser section while the second term is the heat transmitted between the evaporator section and the condenser section.

Table 1: Thermal resistances of the heat balance equations (P. Gang; F. Huide; Z. Tao and J. Jie 2011)

Thermal Resistance	Equation
Thermal resistance between the base panel and the ambient air, $R_{b,a}$	$R_{b,a} = \left( \frac{1}{h_a} + \frac{\delta_{ins}}{K_{ins}} \right) \frac{1}{A_{bi}}$
Thermal resistance between the aluminum plate and the heat pipe, $R_{p,b}$	$R_{p,b} = \frac{\delta_{p,b}}{K_p * A_{p,b}}$
Total thermal resistance of the heat transferred between the evaporator section and the condenser section, $R_{eva,con}$	$R_{eva,con} = R_{eva,p} + R_{con,p} + R_{eva,wick} + R_{con,i}$
The conduction resistance across the pipe wall of the evaporator section of the heat pipe, $R_{eva,p}$	$R_{eva,p} = \frac{\ln(D_{eva,o} / D_{eva,i})}{2\pi L_{eva,p} K_p}$
The conduction resistance across the pipe wall of the condenser section of the heat pipe, $R_{con,p}$	$R_{con,p} = \frac{\ln(D_{con,o} / D_{con,i})}{2\pi L_{con,p} K_p}$
The conduction resistance across the wick of the heat-pipe evaporator, $R_{eva,wick}$	$R_{eva,wick} = \frac{\ln(D_{eva,o} / D_{eva,i})}{2\pi L_{eva,p} K_{wick}}$
The thermal resistance associated with the condensing process, $R_{con,i}$	$R_{con,i} = \frac{1}{\pi D_{con,i} L_{con} h_{con,i}}$ <p>Where</p> $h_{con,i} = 1.13 \left[ \frac{g \sin \theta \rho_l (\rho_l - \rho_v) k_l^3 h_{fg}}{\mu_l \Delta T_{cr} L_{con}} \right]^{1/4}$ <p>(F. P. Incropera, 2013)</p>

Thermal Resistance	Equation
The thermal resistance between the condenser section of the heat pipe and air, $R_{con,a}$	$R_{con,a} = \frac{1}{h_a A_{con,a}}$

## B. Discretization of equations and numerical methodology of the heat pipe model

Since the plate temperature is non-uniform across the x-direction because of the heat pipe and non-heat pipe nodes, it is essential to discretize it in x-direction (along the plate width) as shown in Fig. 2. The longitudinal (along heat pipe evaporator section) and normal (across plate thickness) directions of the plate are lumped and the 1-D steady thermal resistance concept is used. This is justified since the heat pipe condenser and the evaporator sections have uniform temperature along their axial direction while the aluminum plate has high thermal conductivity and very small thickness resulting in almost uniform temperature across the plate. These assumption and methodology were also used by Gang et al. (P. Gang; F. Huide; Z. Tao and J. Jie 2011) and Sweidan et al. (P. Gang; F. Huide; Z. Tao and J. Jie 2011). Equations (5)-(8) shows the discretized form of the mathematical formulations:

For the heat pipe node:

$$K_b * \delta_b * A_{bi} \frac{(T_{b,i+1} - 2T_{b,i} + T_{b,i-1}))}{\Delta x^2} + \frac{T_{ambient} - T_{b,i}}{R_{base,air}} + \frac{T_{p,eva,j} - T_{b,i}}{R_{p,b}} + \frac{T_{skin} - T_{b,i}}{R_{contact}} * A_{bi} = 0 \quad (5)$$

For the non-heat pipe node:

$$K_b * \delta_b * A_{bi} \frac{(T_{b,i+1} - 2T_{b,i} + T_{b,i-1}))}{\Delta x^2} + \frac{T_{ambient} - T_{b,i}}{R_{base,air}} + \frac{T_{skin} - T_{b,i}}{R_{contact}} * A_{bi} = 0 \quad (6)$$

For the evaporator section:

$$\frac{(T_{b,i} - T_{\rho,eva,j})}{R_{\rho,b}} + \frac{(T_{\rho,con,j} - T_{\rho,eva,j})}{R_{eva,con}} = 0 \quad (7)$$

For the condenser section:

$$\frac{(T_{\rho,eva,j} - T_{\rho,con,j})}{R_{eva,con}} + \frac{(T_{ambient} - T_{\rho,con,j})}{R_a} = 0 \quad (8)$$

The differential node (i) corresponds to the heat pipe node and the non-heat pipe node on the base panel and the differential node (j) corresponds to the node on the heat pipe itself. The algorithm input variables are the assumed back skin temperature, the heat pipe and the base panel dimensions as well as the thermal and physical properties. Starting with initial assumption for the base panel, the evaporator, and the condenser temperature the heat pipe model undergoes an iterative process to solve for the base panel temperature. Iterations are achieved until convergence such that all energy equations are conserved in each grid and the maximum relative error between the new and old temperatures is about  $10^{-6}$ . The convergence is usually attained after 48,241 iterations during less than 2 minutes for the heat pipe model. The grid size ensures converged grid independent solution when using central differencing for the second order terms accounting for the conduction heat transfer in the base panel zone. The width of the base panel is 30 cm and is divided into N grids of size  $\Delta x = 5$  mm. The numerical solution is repeated for different grid sizes to ensure that a grid-independent solution is obtained. The mathematical formulation is solved by developing a code using the Matlab software. The algorithm of the heat pipe model integrated with the bio-heat model is shown in Fig. 3.

### **C. Integration of the bio-heat model with the heat pipe model**

The developed approach in this work uses the back skin temperature as an input value. Nevertheless, in real life scenario, the skin temperature changes depending on the ambient conditions, clothing resistance, the body segment, and the metabolic rate. Consequently, In order to find the exact back skin surface temperature, a bio-heat model must be coupled with the heat pipe model. In this study, the human body is in a seated posture; therefore, there is a non-uniformity in ambient condition for the back segment that is in contact with the chair. To account for this non-uniformity, Othmani et al. model (M. Al-Othmani; N. Ghaddar and K. Ghali, 2008) was adopted. Indeed, the bio-heat model of Othmani et al. (M. Al-Othmani; N. Ghaddar and K. Ghali, 2008) divides the human body into 15 segments: head, chest, upper arms, forearms, hands, thighs, calves, and feet. Each body segment is represented by one core node, six angular skin nodes, one artery blood node, and one vein blood node. The six angular skin nodes are used to take into account the non-uniform environment that surrounds the human body segments. For our case, the chest is not exposed completely to the ambient conditions: part of the segment is in direct contact with the chair. Therefore, three skin nodes out of six represent the contact part of the chest. For these nodes, the contact resistance of the back with the chair is measured experimentally according to Han et al. (T. Han; L. Huang; S. Kelly; C. Huizenga and Z. Hui) (see the experimental section).

In general, the inputs to the bio-heat model are the metabolic rate, the clothing properties, contact resistance, and the ambient conditions. The metabolic rate depends on the human activity which is usually 1 MET for a seated person (B. Ainsworth; W. Haskell; M. Whitt; M. Irwin; A. Swartz; S. Strath and A. Leon, 2000). The thermal properties of the fabric type play an important role in the heat transfer between the environment and the skin. The prediction of occupant thermal



comfort was evaluated using the models proposed by Zhang et al. (H. Zhang; E. Arens; C. Huizenga and T. Han, 2010). The thermal comfort ranged from -4 (very uncomfortable) to +4 (very comfortable). In the same manner, the thermal sensation scaled from -4 (very cold) to +4 (very hot).

A flow chart of the coupling method between the heat pipe and bio-heat models is shown in Fig. 3. As a first step, the back skin temperature is assumed in the heat pipe model and the base panel temperature is estimated based on this assumption (see Fig. 3). Afterwards, all the inputs are set appropriately in the bio-heat model and the back skin temperature calculated is integrated into the heat-pipe model. Then, the new base panel temperature is obtained by the heat pipe model and entered into the bio-heat model to predict the new back skin temperature. This iterative process is repeated until convergence is reached. The number of iterations depends on the initial temperature guess of the skin. Convergence is attained when the relative error of skin temperature is less than  $10^{-6}$ .

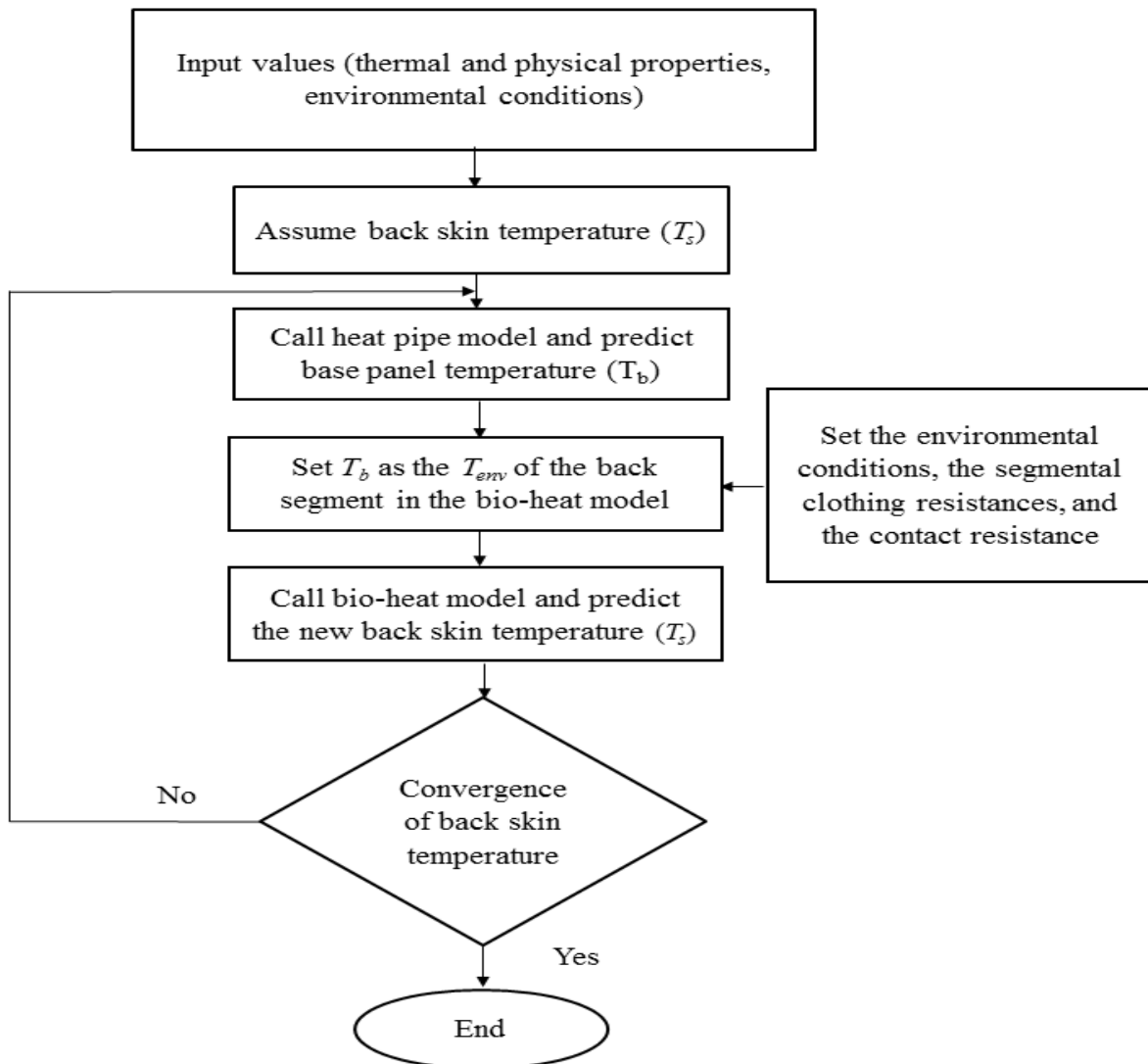


Fig. 3. Flow chart of the coupling methodology

## CHAPTER III

### EXPERIMENTAL METHODOLOGY

The aim of the experiment is (i) to determine the contact resistance between the non-uniform body segment and the chair, and (ii) to validate the heat pipe model predictions of the base panel.

#### A. Experimental Setup

The experiments were conducted in a controlled environmental chamber set at  $22\text{ }^{\circ}\text{C} \pm 0.7\text{ }^{\circ}\text{C}$  with a relative humidity of  $50\% \pm 2.5\%$ . The thermal manikin “Newton” represented in Fig. 4 is manufactured by the Northwestern measured technology (Epoxy Thermal Manikin) and placed on the car seat in the environmental chamber. “Newton” can report the surface temperature for 20 segments based on assigned constant heat flux with a maximum heat flux of  $700\text{ W/m}^2$ . The thermal manikin is controlled through “ThermDAC” control software that reports the temperature of all the body segments. However, the temperatures of the heat pipes and the base panel were measured using K-type thermocouples with accuracy of  $\pm 0.3\text{ }^{\circ}\text{C}$ . The thermal manikin was clothed with a pant (75% cotton, 25% polyester) and long sleeved cotton shirt (100% cotton) having a dry resistance of  $0.041\text{ K}\cdot\text{m}^2/\text{W}$  and  $0.046\text{ K}\cdot\text{m}^2/\text{W}$ , respectively. The dry resistance was measured by a dry thermal manikin test following ASTM F 1291 standard method (ASTM international standard).

The geometry of the heat pipe manufactured by CRS Engineering (CRS Engineering) is represented in Fig. 5. A grooved wick structure is placed along the inner diameter of the heat pipe which generates capillary pressure that returns the condensate liquid back to the evaporator section. The heat pipe used is made of copper and the working fluid is pure water. According to CRS Engineering, the working fluid evaporates at any temperature above  $5\text{ }^{\circ}\text{C}$  up to the

maximum operating temperature (150 °C). The thermal properties are summarized in Table 2 (M. Esen, 2003) (P. Gang; F. Huide; Z. Tao and J. Jie 2011). The base panel has an overall dimension of 40 cm × 30 cm × 0.1 cm with a thermal conductivity of 237 W/m·K and it was insulated using a 0.5 cm fiberglass insulation layer.

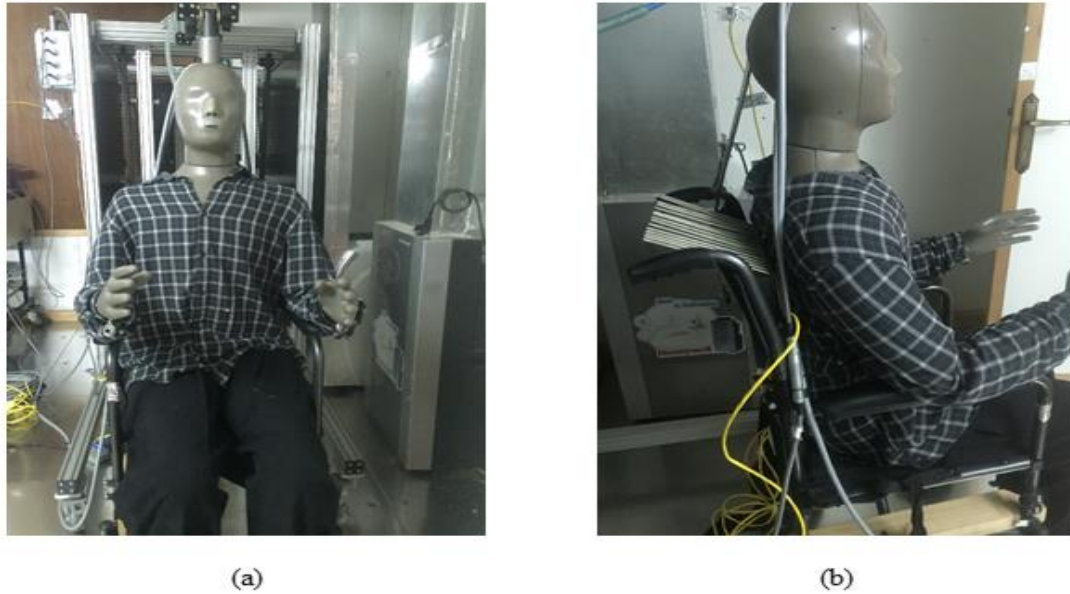


Fig. 4. (a) Front View of the thermal manikin (b) Side view of the thermal manikin

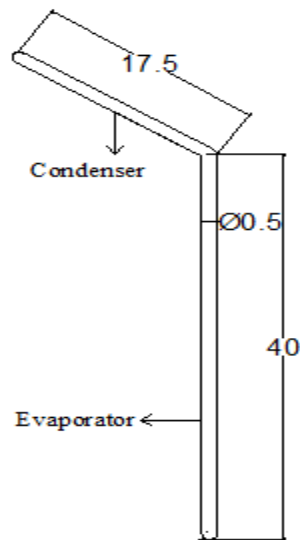


Fig. 5. Manufactured heat pipe geometry

## B. Contact resistances measurement

The objective of this experiment is to determine the contact resistance of the back with the chair. The thermal manikin was placed in upright position with a straight back. The experiment was conducted in an environmental chamber set at  $22\text{ }^{\circ}\text{C} \pm 0.7\text{ }^{\circ}\text{C}$  with a relative humidity of  $50\% \pm 2.5\%$ . A constant heat flux mode of  $25\text{ W/m}^2$  was assigned for all the body segments of the thermal manikin. After steady state condition was reached, the temperature of the back and the chair were recorded. Then, the contact resistance is determined by the following correlation:

$$R_{contact} = \frac{T_s - T_b}{q_{back}} \quad (9)$$

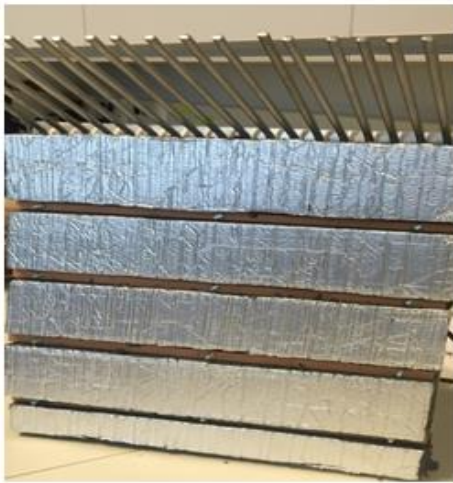
## C. Experimental protocol for the heat pipe system

The experiments were performed with and without the installation of the heat pipe system to assess its effectiveness in reducing the base panel temperature. Twenty heat pipes were attached to the aluminum plate from the evaporator section by using (i) a thermal grease that expels air to ensure a direct contact between the heat pipe and the aluminum plate (ii) a wooden support for fixation purpose as shown in Fig. 6(a) and Fig. 6(b). The assembly is fixed to the car seat by using a clamp support. The evaporator heat pipe section is insulated from the car seat side and from the lateral parts to assure good heat transfer from the back to the heat pipe. The condenser section is exposed to the environment where heat is exchanged through natural convection. In the case of no heat-pipe experiment, the aluminum plate is directly attached to the car compartment. To run the experiment, the room was set to  $22\text{ }^{\circ}\text{C} \pm 0.7\text{ }^{\circ}\text{C}$  with a relative humidity of  $50\% \pm 2.5\%$ . After setting the experimental ambient conditions, the thermal manikin was turned on and initialized to be at the thermo-neutral state. The temperature of the back in the experimental setup was set to  $34\text{ }^{\circ}\text{C}$ . The base panel temperature was monitored continuously until reaching

stabilized values which occurred within an experimental period of 90 minutes. The experimental base panel temperature is then compared with the simulations performed for the heat pipe model.

Table 2: Thermal properties of the heat pipes

Property/Parameter	Value
Vapor pressure at boiling point (5 °C)	0.0084 bar
conductivity of heat pipe, $\kappa_p$	410 W/K·m
Conductivity of the fluid, $k_l$	0.578 W/m·k
Density of the liquid, $\rho_l$	1000 kg/m <sup>3</sup>
Density of the vapor, $\rho_v$	0.00645 kg/m <sup>3</sup>
Viscosity of the fluid, $\mu_l$	1537×10 <sup>-6</sup> Pa·s
heat of vaporization, $h_{fg}$	2491.9 kJ/kg



(a)



(b)

Fig. 6. Heat pipe assembly (a) with the insulation layer (b) without the insulation layer

## CHAPTER IV

### Results and Discussions

#### A. Validation of the heat pipe model with experimental data.

The validation of the heat pipe model was performed by comparing the experimental data obtained from the thermal manikin experiment. The inputs to the heat pipe model are the back skin temperature, the contact resistance of the back determined experimentally, and the ambient conditions. The contact resistance of the back determined experimentally is  $0.133 \pm 0.001$  K·m<sup>2</sup>/W and is based on repeated experiments under same ambient and body posture (sitting with upright back). Table 3 presents the predicted and the experimental values of the base panel temperature with and without heat pipe. It is obvious that the temperature of the base panel decreased from 32.2 °C without heat pipes to 28.4 °C with heat pipes. This is due to the improvement in the convective currents and the increase in the heat absorbed by the heat pipes which is then released by natural convection at the condenser section. The difference in temperature between the nodes was less than (0.2 °C) since the base panel has high thermal conductivity and the distance between the nodes is very small (5mm) and hence only the average temperature along the plate width is presented. The results showed good agreement between predicted and measured base panel temperature with a maximum relative error of 4.2%.

Table 3: Temperature of the base panel evaluated experimentally and theoretically with and without heat pipe

Base Panel Temperature	With heat pipe (Standard deviation)	Without heat pipe (Standard deviation)
Experimental results (°C)	27.8 ( $\pm 0.5$ °C)	30.9 ( $\pm 0.5$ °C)
Simulation results (°C)	28.47	32.2

## B. Integrated bio-heat model and heat pipe model

In order to determine the physiological response of the human body, the heat pipe model is integrated with a bio-heat model (M. Al-Othmani; N. Ghaddar and K. Ghali, 2008) to come up with the back skin temperature, thermal comfort, and thermal sensation of the human body for a certain environmental conditions. The inputs used to the bio-heat model are the ambient conditions, the metabolic rate, clothing resistance and the contact resistance. The room was set at 22 °C with a relative humidity of 50 % and the metabolic rate for a seated person is 1 MET (B. Ainsworth; W. Haskell; M. Whitt; M. Irwin; A. Swartz; S. Strath and A. Leon, 2000). As for clothing, the same properties reported in the experimental set-up section are used. The contact resistance of the back is  $0.133 \pm 0.001 \text{ K}\cdot\text{m}^2/\text{W}$  determined experimentally. The predicted back skin temperature, the local thermal comfort and sensation are shown in Table 4.

Table 4: Results of the back skin temperature, local thermal comfort, and the thermal sensation with and without heat pipe

Simulated Case	Base panel temperature (°C)	Back skin temperature (°C)	Local thermal comfort	Local thermal sensation
With heat pipe	28.82	34.107	2.405	0.131
Without heat pipe	32.2	35.105	0.188	1.189

It is clear that both the base panel and back skin temperatures decreased when the heat pipe system was incorporated where the back decreased from 35.105 °C without heat pipe system to 34.107 °C with heat pipe system, and the base panel temperature decreased from 32.2 °C without heat pipe system to 28.82 °C with heat pipe system. Moreover, the local thermal comfort and



thermal sensation has improved when the heat pipe system was incorporated. The local thermal comfort of the back increased from 0.188 to 2.405 which mean that the back is very comfortable. However, the local thermal sensation of the back decreased from 1.189 to 0.131 which corresponds for a neutral state.

### **C. Parametric study using validated bio-heat model and heat pipe model**

The integrated model results showed a clear dependence of segmental back skin temperature, base panel temperature, thermal comfort, and thermal sensation on the variation of the number of heat pipes. Therefore, it is of interest to find the optimal number of heat pipes that ensure the local comfort of the human back. This is achieved by conducting a parametric study that takes a common passenger conditions, finds the improvement in back sensation and comfort with the implementation of the heat-pipe system, and comes up with the needed heat pipe number that results in good back local thermal sensation and comfort and improved overall comfort.

According to ASHREA Standard 55 (R. Dear and G. Brager, 2002), the local comfort and thermal sensation are exclusively influenced by four environmental factors (temperature, thermal radiation, humidity and air speed), and two personal factors (activity and clothing resistance). In this case study, these parameters are taken from the reported data of Musat et al. (R. Musat, and E. Helerea, 2009), Hosni et al. (M. Hosni; Y. Guan; B. Jones and T. Gielda, 2003), Danca et al. (P. Danca; A. Vartires and A. Dogeanu, 2016), and Cena et al. (K. Cena and R. Dear, 2001). According to Musat et al. (R. Musat, and E. Helerea, 2009), average operating conditions in car cabins are (i) air temperature of 22 °C; (ii) average air velocity of 0.13 m/s; (iii) relative humidity of 50 %; and (iv) mean radiant temperature of 22 °C. Although Musat et al. (R. Musat, and E. Helerea, 2009) reported that at these conditions, the passenger is in a comfort state, he does not testify the local comfort of the passenger. Indeed, overall comfort does not imply that the local

comfort of each human segment is achieved. Therefore, it is of interest to investigate the local thermal comfort and sensation of the passenger at these reported conditions for heat pipe and non-heat pipe system.

The personal factors are specified according to the performed activity and to the weather. For a seated person, the metabolic rate is 1 MET (B. Ainsworth; W. Haskell; M. Whitt; M. Irwin; A. Swartz; S. Strath and A. Leon, 2000), and the recommended summer clothing insulation is  $0.0775 \text{ K}\cdot\text{m}^2/\text{W}$  at approximately  $23 \text{ }^\circ\text{C}$  (K. Cena and R. Dear, 2001). The thermal comfort and the sensation of the back are compared using the scales of the Model of Zhang et al. (H. Zhang; E. Arens; C. Huizenga and T. Han, 2010). The selection of the optimum number of heat pipe was performed by comparing the back skin surface temperature, the base panel temperature, the local sensation as well as the local thermal comfort for different number of heat pipes. The base case was considered as the one without the embedded heat pipes. Afterwards, the number of heat pipes is incremented by 3 with a minimum of 5 and a maximum of 23.

Table 5 summarizes the predictions of the simulation model of the temperatures of the back and the base panel as a function of the number of heat pipes. The temperature of the base panel decreased from  $32.2 \text{ }^\circ\text{C}$  without heat pipes to  $28.88 \text{ }^\circ\text{C}$  with 20 heat pipes. Similarly, the temperature of the back skin surface decreased from  $34.92 \text{ }^\circ\text{C}$  without heat pipes to  $34.26 \text{ }^\circ\text{C}$  with 20 heat pipes. When using more than 17 heat pipes, the temperature of the base panel as well as the temperature of the back showed no significant change. This implies that the optimum number of heat pipes that is capable of cooling the back is 17 since there was no significant change after this number. The local thermal sensation and comfort were also evaluated for the calculated back temperatures (H. Zhang; E. Arens; C. Huizenga and T. Han, 2010) as a function of the number of heat pipes and for the base case as shown in Fig.7. It is observed from Fig. 7 (a)

that the local thermal sensation of the back improved from a warm state (1.156) without heat pipes to a neutral state (0.335) with 17 heat pipes. Moreover, the local thermal comfort of the back enhanced from a neutral state (0.241) without heat pipes to very comfortable state (2.20) with 17 embedded heat pipes. At higher than 17 heat pipes, the local sensation as well as the local thermal comfort didn't show a significant change with increasing the number of heat pipes. Considering the overall thermal comfort as a function of the number of heat pipes shown in Fig. 7 (b), it is clear that it increased from 0.929 without heat pipe to 1.182 with 17 heat pipes. This implies that a local cooling method enhances slightly the overall thermal comfort of the passenger. Therefore, it can be concluded that using 17 embedded heat pipes is optimal and the system is capable of cooling the back and providing good sensation with very comfortable state.

Table 5: Temperature of the base panel and the back skin surface as a function of the number of heat pipes

Number of heat Pipes	0	5	8	11	14	17	20	23
Temperature of base panel (°C)	32.20	30.70	30.16	29.68	29.26	28.88	28.53	28.53
Temperature of back skin (°C)	34.92	34.56	34.47	34.39	34.32	34.26	34.20	34.20

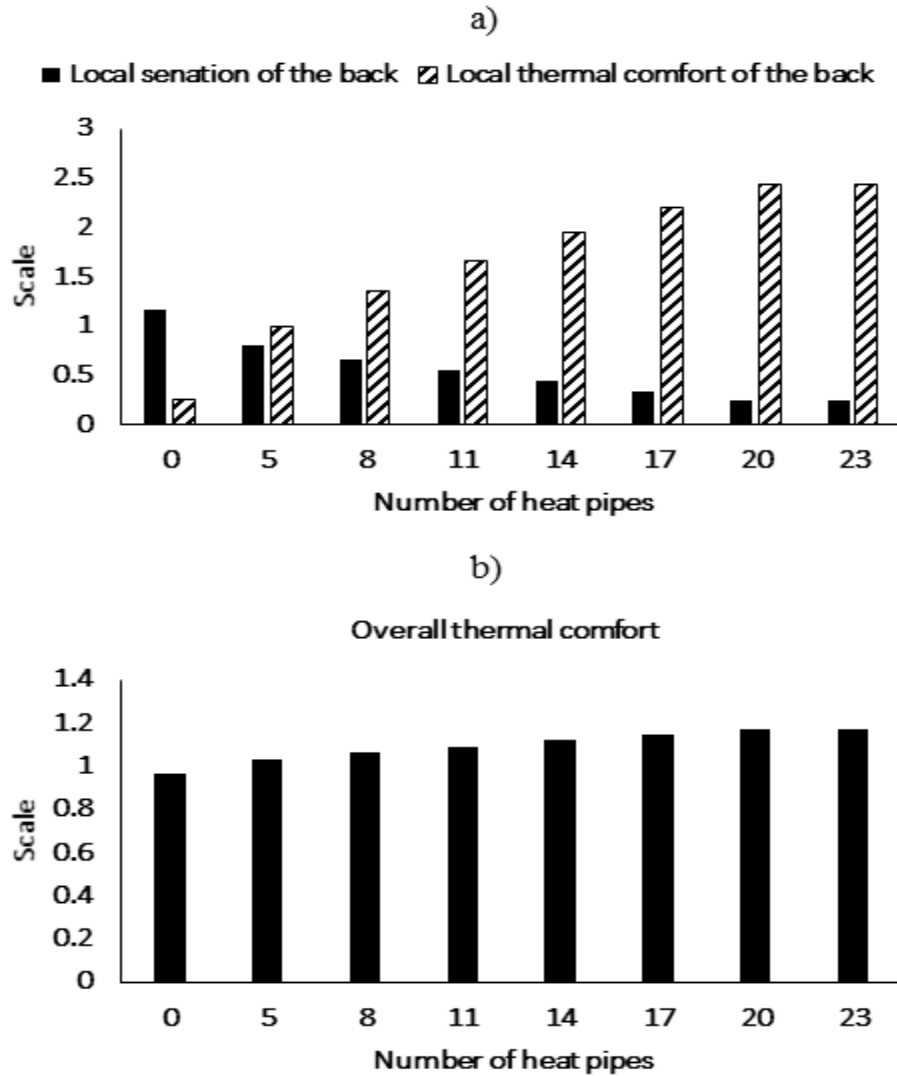


Fig. 7 Results as a function of the number of heat pipe (a) Local thermal comfort and local thermal sensation of the back (b) Overall thermal comfort

#### D. Conclusion

In this study, a passive cooling system installed in the car seat to cool the human back is studied. The system is composed of heat pipes embedded in the car seat in contact with the passenger's back. The mathematical formulation was developed to predict the performance of the system. The model predictions of back and base panel temperature were validated by experiments on a

heated thermal manikin. The heat-pipe model is integrated with a bio-heat model in order to simulate the human thermal response with and without the implementation of the suggested system. It was found that implementing the heat-pipe system resulted in a decrease in the back and the base panel temperatures of about 1°C and 4 °C, respectively. Moreover, it was shown that the local thermal comfort and thermal sensation have improved when the heat pipe system was incorporated.

Finally, a parametric study using a realistic passenger environment in car was performed to determine the optimum number of heat pipes that can provide a state of thermal comfort. The results revealed that as the number of heat pipe increased, the back skin temperature as well as the base panel temperature decreased while the back thermal sensation, back thermal comfort, and the overall comfort improved. It was also shown that the optimum number of heat pipe that is able to cool the back and provide a state of thermal comfort is 17 heat pipes. Future work will address the impact of such system on energy performance of the car cooling system and will consider design improvements via actual human subject tests.

## Bibliography

Zhang, H., Arens, E., Huizenga, C., & Han, T. (2010). *Thermal sensation and comfort models for non-uniform and transient environments, part III: Whole-body sensation and comfort. Building and Environment*,45(2), 399-410. doi:10.1016/j.buildenv.2009.06.020

Lindsay, R. A. (1977). *U.S. Patent No. 4,060,276. (n.d.). Washington, DC: U.S. Patent and Trademark Office.*

Zhang, H., Arens, E., Huizenga, C., & Han, T. (2010). *Thermal sensation and comfort models for non-uniform and transient environments, part III: Whole-body sensation and comfort. Building and Environment*,45(2), 399-410. doi:10.1016/j.buildenv.2009.06.020

Itani, M., Ouahrani, D., Ghaddar, N., Ghali, K., & Chakroun, W. (2016). *The effect of PCM placement on torso cooling vest for an active human in hot environment. Building and Environment*,107, 29-42. doi:10.1016/j.buildenv.2016.07.018

Hweij, W. A., Ghaddar, N., Ghali, K., & Habchi, C. (2016). *Optimized performance of displacement ventilation aided with chair fans for comfort and indoor air quality. Energy and Buildings*,127, 907-919. doi:10.1016/j.enbuild.2016.06.052

Cotter, J. D., & Taylor, N. A. (2005). *The distribution of cutaneous sudomotor and alliesthesial thermosensitivity in mildly heat-stressed humans: an open-loop approach. The Journal of Physiology*,565(1), 335-345. doi:10.1113/jphysiol.2004.081562

Rock, M., Dionne, E. P., Haryslak, C., Lie, W. K., & Vainer, G. (2007). *U.S. Patent No. 7,217,456. (n.d.). Washington, DC: U.S. Patent and Trademark Office.*

Zheng, W., & Guo, Z. Y. (2012). *U.S. Patent No. 13/648,763. (n.d.). Washington, DC: U.S. Patent and Trademark Office.*

Chen, S., & Yang, J. (2016). *Loop thermosyphon performance study for solar cells cooling. Energy Conversion and Management*,121, 297-304. doi:10.1016/j.enconman.2016.05.043

Azad, E. (2008). *Theoretical and experimental investigation of heat pipe solar collector. Experimental Thermal and Fluid Science*,32(8), 1666-1672. doi:10.1016/j.expthermflusci.2008.05.011

Vasiliev, L., Lossouarn, D., Romestant, C., Alexandre, A., Bertin, Y., Piatsiushyk, Y., & Romanenkov, V. (2009). *Loop heat pipe for cooling of high-power electronic components. International Journal of Heat and Mass Transfer*,52(1-2), 301-308. doi:10.1016/j.ijheatmasstransfer.2008.06.016

Sweidan, A., Ghaddar, N., & Ghali, K. (2016). *Optimized design and operation of heat-pipe photovoltaic thermal system with phase change material for thermal storage. Journal of Renewable and Sustainable Energy*,8(2), 023501. doi:10.1063/1.4943091

- Wu, X. P., Johnson, P., & Akbarzadeh, A. (1997). Application of heat pipe heat exchangers to humidity control in air-conditioning systems. *Applied Thermal Engineering*, 17(6), 561-568. doi:10.1016/s1359-4311(96)00058-0
- Chaudhry, H. N., & Hughes, B. R. (2014). Climate responsive behaviour of heat pipe technology for enhanced passive airside cooling. *Applied Energy*, 136, 32-42. doi:10.1016/j.apenergy.2014.09.017
- Salloum, M., Ghaddar, N., & Ghali, K. (2007). A new transient bioheat model of the human body and its integration to clothing models. *International Journal of Thermal Sciences*, 46(4), 371-384. doi:10.1016/j.ijthermalsci.2006.06.017
- Al-Othmani, M., Ghaddar, N., & Ghali, K. (2008). A multi-segmented human bioheat model for transient and asymmetric radiative environments. *International Journal of Heat and Mass Transfer*, 51(23-24), 5522-5533. doi:10.1016/j.ijheatmasstransfer.2008.04.017
- Gang, P., Huide, F., Tao, Z., & Jie, J. (2011). A numerical and experimental study on a heat pipe PV/T system. *Solar Energy*, 85(5), 911-921. doi:10.1016/j.solener.2011.02.006
- Incropera, F. P. (2013). *Fundamentals of heat and mass transfer*. Hoboken, NJ: Wiley.
- Han T, Huang L, Kelly S, Huizenga C, Hui Z. *Virtual Thermal Comfort Engineering*. SAE Technical Paper Series 2001. doi:10.4271/2001-01-0588.
- Ainsworth, B. E., Haskell, W. L., Whitt, M. C., Irwin, M. L., Swartz, A. M., Strath, S. J., Leon, A. S. (2000). *Compendium of Physical Activities: an update of activity codes and MET intensities*. *Medicine & Science in Sports & Exercise*, 32(Supplement). doi:10.1097/00005768-200009001-00009
- Zhang, H., Arens, E., Huizenga, C., & Han, T. (2010). Thermal sensation and comfort models for non-uniform and transient environments: Part I: Local sensation of individual body parts. *Building and Environment*, 45(2), 380-388. doi:10.1016/j.buildenv.2009.06.018
- Zhang, H., Arens, E., Huizenga, C., & Han, T. (2010). Thermal sensation and comfort models for non-uniform and transient environments, part II: Local comfort of individual body parts. *Building and Environment*, 45(2), 389-398. doi:10.1016/j.buildenv.2009.06.015
- Epoxy Thermal Manikin, *Instruments for Textile & Biophysical Testing*. Seattle, WA, [http://www.thermetrics.com/sites/default/files/product\\_brochures/Newton%20Manikin%20Thermetrics%202015.pdf](http://www.thermetrics.com/sites/default/files/product_brochures/Newton%20Manikin%20Thermetrics%202015.pdf)
- ASTM F1291-15. ASTM International - Standards Worldwide. <https://www.astm.org/DATABASE.CART/HISTORICAL/F1291-15.htm> (accessed January 6, 2017).
- CRS Engineering. *CRS Engineering - Heat Pipes & Heat Sinks Manufacturers*. <http://www.heat-pipes.com/index.php?sectionid=1> (accessed January 6, 2017).
- Esen M. Thermal performance of a solar cooker integrated vacuum-tube collector with heat pipes containing different refrigerants. *Solar Energy* 2004;76:751-7. doi:10.1016/j.solener.2003.12.009.

Dear, R. J., & Brager, G. S. (2002). *Thermal comfort in naturally ventilated buildings: revisions to ASHRAE Standard 55*. *Energy and Buildings*,34(6), 549-561. doi:10.1016/s0378-7788(02)00005-1

Musat, R., & Helerea, E. (2009). *Parameters and models of the vehicle thermal comfort*. *Acta Universitatis Sapientiae, Electrical and Mechanical Engineering*, 1, 215-226.

Hosni, M. H., Guan, Y. (., Jones, B. W., & Giolda, T. P. (2003). *Quantitative Measurement of Thermal Comfort Under Transient and Non-Uniform Conditions in Vehicles*. *SAE Technical Paper Series*. doi:10.4271/2003-01-2232

Danca, P., Vartires, A., & Dogeanu, A. (2016). *An Overview of Current Methods for Thermal Comfort Assessment in Vehicle Cabin*. *Energy Procedia*,85, 162-169. doi:10.1016/j.egypro.2015.12.322

Cena, K., & Dear, R. D. (2001). *Thermal comfort and behavioural strategies in office buildings located in a hot-arid climate*. *Journal of Thermal Biology*,26(4-5), 409-414. doi:10.1016/s0306-4565(01)00052-3